

DENSE CORES OF INTERSTELLAR MOLECULAR GAS

Francesca Pinna

Facultat de Física, Universitat de Barcelona, Martí i Franqués 1, 08028 Barcelona, Spain.

ABSTRACT

From the analysis of real observation data concerning the $(J, K) = (1, 1)$ and $(J, K) = (2, 2)$ inversion transitions of the ammonia molecule, I estimated the physical parameters for the molecular cloud L1228. First of all, I identified the lines of interest in twelve different spectra, measured in a twelve-point grid which also allowed me to outline a map of the dense region. Secondly, by means of the maximum intensity and the FWHM of the transition lines, after being fitted to a gaussian distribution, I characterized the $(J, K) = (1, 1)$ transition by the optical depth and the excitation temperature. Lastly, I found some important properties of the condensation such as its size, the kinetic temperature and the column and volume densities leading to two different values of the mass whose discrepancy confirmed that the region is not optically thin. Comparing my results for the clump mass with the virial mass, I was able to state the approximate equilibrium of the dense core of L1228.

Key words. ISM: NH₃ molecules - emissions: NH₃ inversion transitions - physical properties: mass - physical conditions: virial equilibrium

I. INTRODUCTION

The NH₃ molecule traces the dense core of a hydrogen molecular interstellar cloud, where new stars are formed by gravitational collapse. Together with both molecular and optical outflows, ammonia emissions are the key to study the earliest stages of stellar evolution. On the one hand, the distribution of high density tracers, such as NH₃ and CS, suggests the position of young stellar objects (YSO), which are usually located near the emission peak. On the other hand, outflows trace the mass losses related to the formation of a new protostar and they give a hint about the evolution phase in which it finds itself [3]. Molecular outflow (in the radio domain) is one of the earliest observable stages of evolution, it is usually associated with ammonia emission and it is typical of stellar objects younger than the ones with detectable optical outflows (as Herbig Haro objects). NH₃ column density, which is to say the high density of the YSO surrounding matter, decreases whereas the gas is being swept up by the outflow, until the optical radiation is allowed to escape [11].

The NH₃ molecule is relatively abundant in molecular clouds and easy to find ([6], page 90), but its rotational transitions, related to the rotation of the molecule as a whole, would be in the infrared domain, far from the available energies in cold clumps. Nevertheless the peculiar molecular structure makes each level split into two inversion levels, whose transitions now correspond to the centimetric range and to the typical energy exchanges in this kind of regions. Therefore, the inversion transitions are of enormous interest for studying the interstellar medium. The most remarkable advantage of using ammonia observations is that, thanks to its hyperfine structure, it is possible to obtain a large amount of information and to calculate the most important physical parameters from only one transition, which is to say only one observation. The inversion lines have frequencies enough

similar to each other, and they can be observed with the same instrument and the same angular resolution.

Inversion transitions are due to vibrational motions of the nitrogen's nucleus, which passes through the plane of the three hydrogen atoms by tunnel effect, "inverting" the molecule. The presence of these three hydrogen atoms creates a potential barrier which deforms the molecule potential with respect to a simple harmonic one, so that a maximum appears in the hydrogen atoms plane position. Since the maximum has a higher energy, the nitrogen oscillates around each minimum but sometimes it crosses the plane, resulting in a transition. Each rotational level, defined by the two quantum numbers J (associated to the angular momentum) and K (its projection above the molecule symmetry axis), is splitted into two more levels, with parity $+$ or $-$. The inversion transitions occur between levels of different parity and, depending on the involved levels, they lead to different spectral lines. On both sides of a main line, which is the most intense and it is owed to two transitions with extremely similar frequency, we find four satellite lines, two interior ones and two exterior with respect to the main line position (see Fig.(1), Appendix), frequently difficult to detect.

The aim of this study falls in this context and it concerns L1228, a high galactic latitude molecular cloud ($\alpha(J2000) = 20^{\text{h}}57^{\text{m}}13^{\text{s}}.2$, $\delta(J2000) = +77^{\circ}35'46''$ [7]), located between the tail of Ursa Minor and the Cepheus constellation in our sky, lying towards the direction of the Cepheus flare [12]. Regarding the distance, I adopted the value of 300 pc, given by Bally et al. [4]. The region is characterized by a well-collimated bipolar CO outflow, centred on the object IRAS 20582+7724 (detected by Anglada et al. [2]) which is a Class I protostar [5] believed to be the exciting source. In addition, among the several Herbig-Haro objects detected in the same region [4], we find the two giant HH199 and HH200, being the last one's source a T Tauri star [5].

II. RESULTS AND DISCUSSION

A. Spectra analysis: antenna temperature, velocity, map and radius

The observation data which I used in this study, are related to the two most intense NH_3 inversion transitions, $(J, K) = (1, 1)$ and $(J, K) = (2, 2)$, which occur respectively at the frequencies of 23.6944960 GHz and 23.7226320 GHz [3]. They were obtained by Anglada et al. on February 1990 with the 37 m radio telescope at Haystack Observatory, with the purpose of taking an overview of the region, so that the resolution is not high but enough to estimate the physical properties of L1228. The data are, for the $(J, K) = (1, 1)$ transition, twelve different spectra measured in a 3x4-point grid around the IRAS source position, which was expected to correspond to the emission peak of ammonia. Concerning the $(J, K) = (2, 2)$ transition, only one spectrum was taken since the line is weaker and it is more difficult to detect the emission out of the central position. The beam size of the telescope was 1'4 at the observed frequencies, thus this was also the distance between the grid points, and the main beam efficiency was 0.32 [7].

The spectra were already reduced using the CLASS package, developed by Forveille, Guilloteau and Lucas (1989) [11]. The frequency in the abscissa axis was already changed to the radial velocity (in km s^{-1}) with respect to the local standard of rest, given that a frequency shift can be always associated to a Doppler non-relativistic velocity. The antenna temperature in Kelvins was presented in the ordinate axis (see Fig.(1), Appendix).

My first step was to identify the lines of interest, first of all the main line of each spectrum and then the interior satellite lines only for the $(1, 1)$ spectrum in the central position. The fortran programme `gauss.f`, created by Robert Estalella in 1998 and updated in 2004, fits to gaussian distributions iteratively by least squares method. By means of this programme, I could fit the lines thanks to the fact that their expected profiles had to be almost gaussian, since the particles approximately follow a Maxwellian velocity distribution ([6], page 13). From the adjustments, I found the data shown in Table I (see the Appendix) for antenna temperature T_A in K, line width ΔV (as FWHM) in km s^{-1} and line position V_0 in km s^{-1} . Each line is identified in the table by the transition (J, K) it corresponds to, its position in the spectrum (main or interior satellite line i.s.l.) and the position where the spectrum was taken with respect to the IRAS object, in arcminutes.

In relation to the uncertainties associated with the results presented in this work, I considered the gaussian adjusting errors (presented in Table I) and propagated them in the standard way. The identification of the main line in the peripheral positions was sometimes difficult due to the weakness of the signal, but made possible by the fact that all the main lines had to be around the same velocity position. Relative errors increase moving away

from the central (spatial) position and in particular, for the (1'4,-2'8) position, the line peak was confused with noise and the goodness of the measurement was too poor. In this case, I estimated an upper limit for T_A as a noise peak.

The central velocity V_0 of the line is generally around the negative value of -8 km s^{-1} , which indicates a global radial velocity of the cloud core towards us and means a frequency blueshift. Nevertheless, the central velocity of the main line is not exactly the same for all spectra, but its absolute value is smaller or larger depending on the position in the grid. This indicates that different regions have their own different velocities relatively to the rest of the clump. In spite of not having data with enough resolution to study directly the velocity shifts, from other tracers observations it is known that velocity follows a pattern given by the CO bipolar outflow, so that the dense core suffers from a disruption [12].

My first result about the condensation is the contour map in Fig.(2) (see the Appendix), drawn by means of the fortran programme `mapa.f`, also created by Robert Estalella (1998-2004). The programme computes, from the intensity in the twelve-point grid, new levels by cubic interpolation. The map proves how, by quantifying ammonia emission in several points, it is possible to map easily the high density region. It appears to be elliptic and it approximately accords with the position of the IRAS source coinciding with the emission peak. Furthermore, comparing my map with CO maps in references, as the one in [4], NH_3 emission distribution proves to be perpendicular to the bipolar outflow. The map gave me the possibility to estimate the radius R in parsecs of the dense core, as the geometrical average of the major (a) and the minor (b) semi-axis of the half intensity contour and taking into account the distance of L1228 from us:

$$\begin{aligned} a &= (0.136 \pm 0.004) \text{ pc} \\ b &= (0.087 \pm 0.003) \text{ pc} \\ R &= (0.1090 \pm 0.0002) \text{ pc} \end{aligned}$$

B. Characterization of the $(J, K) = (1, 1)$ transition

In all the following calculations I used the brightness temperature, obtained by dividing the antenna temperature to the telescope's main beam efficiency. In relation to satellite lines temperature, I adopted the arithmetic average of left and right lines.

In order to calculate the optical depth of the $(1, 1)$ transition, I needed to know the one of the main line

$$\tau_m = 1.5 \pm 0.1$$

which I computed numerically by a simple fortran code, using the false position method, applied to the following equation:

$$\frac{T_L(1, 1; m)}{T_L(1, 1; si)} = \frac{1 - e^{-\tau_m}}{1 - e^{-\tau_m/3.6}} \quad (1)$$

where $T_L(1, 1; m)$ and $T_L(1, 1; si)$ are the brightness temperatures, measured in the central position, respectively for the main and the satellite lines ([6], page 94). The total optical depth of the transition can be estimated as twice τ_m [10]:

$$\tau(1, 1) = 3.0 \pm 0.2$$

This is the important evidence of the transition (and then the region in this determined frequency) not being optically thin, because τ is not $\ll 1$, although we are not still in the case of optically thick as τ is not $\gg 1$ ([6], page 8).

The excitation temperature T_{ex} is defined as the temperature for which the source function at the given frequency is equal to the Planck function ([6], page 9) and can be evaluated by the radiative transport equation

$$T_L(1, 1; m) = f [J_{\nu_0}(T_{ex}) - J_{\nu_0}(T_{bg})] (1 - e^{-\tau_m}) \quad (2)$$

where f is the beam filling factor [3], unitary since I supposed that the beam was uniformly distributed in the central position; $T_{bg} = 2.73$ K is the background radiation temperature ([8], page 358). The functions

$$J_{\nu_0}(T) = \frac{h\nu_0/k}{e^{h\nu_0/kT} - 1} \quad (3)$$

are increasing functions of temperature and they indicate the intensity in temperature units, for a given frequency ν_0 . h and k are the Planck and Boltzmann constants [9]. Once I had the excitation temperature,

$$T_{ex} = (6.6 \pm 0.2)\text{K}$$

I calculated the column density at the rotational level (1, 1) in the following way:

$$N(1, 1) = \frac{16\pi\nu_0^3}{c^3 A_{+-}} \frac{e^{h\nu_0/kT_{ex}} + 1}{e^{h\nu_0/kT_{ex}} - 1} \tau_m \Delta v \quad (4)$$

where $A_{+-} = 1.67 \times 10^{-7} \text{s}^{-1}$ is the spontaneous emission coefficient for the (1, 1) transition ([6], page 94), obtaining

$$N(1, 1) = (2.8 \pm 0.3) \times 10^{14} \text{cm}^{-2}$$

C. Physical parameters: column and volume densities, mass

The kinetic temperature T_k of a cloud is related to collisions, which are responsible for the relative populations of the different metastable levels of NH_3 molecules. The rotational temperature T_{rot} is an excitation temperature defined by the Boltzmann equation for two rotational levels as for example (1, 1) and (2, 2) (see [6] on pages 15 and 95):

$$\frac{N(2, 2)}{N(1, 1)} = \frac{T_L(2, 2)}{T_L(1, 1)} = \frac{g(2, 2)}{g(1, 1)} e^{-[E(2, 2) - E(1, 1)]/kT_{rot}} \quad (5)$$

The energy $E(J, K)$ and the statistical weight $g(J, K)$ of the (J, K) level can be calculated as

$$E(J, K) = h[B J(J+1) + (C - B)K^2] \quad (6)$$

$$g(J, K) = \begin{cases} 4(2J+1), & K \neq \dot{3} \\ 8(2J+1), & K = \dot{3}, K \neq 0 \\ 4(2J+1), & K = 0 \end{cases} \quad (7)$$

where $B = 2.98 \times 10^{11}$ Hz and $C = 1.89 \times 10^{11}$ Hz are the rotational constants for the NH_3 molecule, and $\dot{3}$ means multiple of 3. As I have mentioned in the Introduction, the molecular cloud radiation field normally does not have enough energy to excite transitions between different rotational states (with $\Delta J = \pm 1$), so that molecules are usually trapped in the lowest energy levels (with $J = K$), called *metastable*. Apart from that, collisions make molecules change from a metastable state to another, determining the population of levels. Consequently, what leads to rotational transitions are collisions, directly related to the kinetic temperature which can be then approximated as the rotational temperature. From equation (5) I obtained

$$T_k \simeq T_{rot} = (13.9 \pm 0.4)\text{K}$$

The total column density of NH_3 can be calculated as the sum of the column density of all populated levels ([6], page 95), related to each other by equations similar to (5). I took into account that only metastable levels with $J(=K) \leq 3$ are significantly populated for $T_k \lesssim 30$ K and the expected volumetric density $n < 10^7 \text{cm}^{-3}$. Assuming for the NH_3 -to- H_2 relative abundance the typical value of 10^{-8} for dense clouds [1], I directly achieved the column density of hydrogen, which approximates the one of the condensation:

$$N(\text{H}_2) = (8 \pm 1) \times 10^{22} \text{cm}^{-2}$$

A first value for the mass can be estimated by the surface given by the half intensity contour (Subsection A).

$$M = (10 \pm 1) \times 10^{31} \text{kg} = (49 \pm 7)M_{\odot}$$

On the other hand I gathered the volume density using the *two levels model* (explained in [6] on page 96):

$$n(\text{H}_2) = \frac{A_{+-}}{\gamma_{+-}} \frac{J_{\nu_0}(T_{ex}) - J_{\nu_0}(T_{bg})}{J_{\nu_0}(T_k) - J_{\nu_0}(T_{ex})} \left[1 + \frac{J_{\nu_0}(T_k)}{h\nu_0/k} \right] \quad (8)$$

where $\gamma_{+-} = 2.27 \times 10^{-11} T_k^{1/2} \text{s}^{-1}$ is the disexcitation coefficient for collisions with H_2 . Then,

$$n(\text{H}_2) = (1.3 \pm 0.1) \times 10^4 \text{cm}^{-3}$$

This model is a good approximation in the thermalized limit ([6], page 19), when the medium density is sufficiently high ($\gg 10^3 \text{cm}^{-3}$) and transitions are predominantly collisional, then the kinetic temperature must be of the same order of the excitation temperature. In our

case, these conditions are fulfilled even if $T_k \sim 2 \times T_{ex}$, which means that some levels are not thermalized.

A new estimation for the cloud mass comes from the volume density, approximating the cloud as a homogeneous sphere of radius R (Subsection A):

$$M = (6.9 \pm 0.7) \times 10^{30} \text{ kg} = (3.5 \pm 0.3) M_{\odot}$$

It is immediate to realize that there is a noticeable discrepancy between the two values found for cloud mass, what I discuss in the next section.

D. A further discussion: mass and equilibrium

The optical depth of the cloud in the frequency of the transition is an important parameter to have an idea of the reliability of the spherical approximation. On the one hand, the column density takes into account all the mass between us and where the radiation comes from, and it is the number of particles in a cylinder with base of one cm^2 and an equivalent height h . Multiplying by a section of the cloud perpendicular to the line of sight, we can obtain the number of particles of the cloud, and then the mass. On the other hand, calculating the mass by the volume density, is equivalent to using the radius instead of the height h . Doing this, more or less information is lost depending on the optical depth, which determines how similar R and h are. In the case of an optically thin region, R and h coincides, giving the same value for the mass. On the contrary, the result I found for the optical depth suggests that I am not in that case, as I explained in the Subsection B. Thus, the volume density gives me only the nearest portion of the cloud and it leads to a result for the mass much lower than what expected from the column density result, which I am then allowed to consider as the good one.

In addition to the distribution of ammonia and outflows, the study of virial equilibrium is of great interest to estimate the phase of evolution of the cloud, giving an idea of the energetic balance. Star formation is related to a gravitational collapse, followed by a new equilibrium when the mass is about the virial mass, related to size and line width as follows ([6], page 126):

$$M_{vir} = \frac{5}{8 \ln 2 G} R (\Delta V)^2 \quad (9)$$

For L1228 condensation I obtained:

$$M_{vir} = (3.7 \pm 0.5) \times 10^{31} \text{ kg} = (19 \pm 2) M_{\odot}$$

A region is usually considered in collapse if its mass exceeds five times the virial mass ([11]). In this case the mass is around twice the virial mass, therefore the core is near virial equilibrium and probably in the final phase of gravitational contraction. Anyway, the gravitational disequilibrium due to the mass excess must be counteracted by additional sources of energy. On the one hand it is likely to be the radiation of the recently formed star,

and on the other hand the (subsonic) turbulent kinetic energy due to macroscopic disordered motions ([6], page 102).

Furthermore, the presence of an embedded YSO causes sometimes local heating effects, which make upper levels (as (2, 2)) be more populated than what I have supposed. As a consequence, the rotational temperature and then the column density appear to be larger ([6], page 96). Lastly, it is important to remark that equation (4) gives an upper limit for the (1, 1) column density, leading to an upper limit for the core mass [11].

III. CONCLUSIONS

I studied the dense core of the dark molecular cloud L1228, by means of ammonia emissions in the centimetric range, related to its inversion transitions. From the line analysis I could map the region and find the most interesting physical properties of the condensation and then reach the following conclusions:

- The map indicates that the dense core has an elliptic shape and a size of around 0.1 pc. The peak of emission is located close to the IRAS source, suggesting that it is the new star recently formed, responsible for the NH_3 excitation. Ammonia density distribution is approximately orthogonal to CO outflow.
- The dense core presents a global velocity towards us but also a different relative velocity in each position where spectra were measured. This accords with a disruption of the nucleus, due to perturbations induced by the CO outflow.
- Kinetic and rotational temperatures are not equal despite the fact that they are of the same order, meaning that the region is not completely thermalized. At the same time the volume density is of the typical order (10^4 cm^{-3}) for a small dark cloud and much larger than the critical density 10^3 cm^{-3} , so that the two levels model is a good approximation.
- The region is not optically thin in the observed frequency. As a result, volume density gives a mass much lower than what column density does, because it is not taking into account all the mass.
- The condensation must be in its final stage of gravitational collapse and there must be appearing other sources counteracting gravity. Two candidates are the radiation that the YSO is starting to emit and the kinetic energy associated with turbulence.

Acknowledgments

I would like to thank both my advisors R. Estalella and R. López for their help, guidance and source material, and I. Sepúlveda for the information provided. I am grateful to my parents, my boyfriend, my sister and my friends for their support during my studies.

APPENDIX

	$R.P.[']$	$T_A[\text{K}]$	$\Delta V[\text{km s}^{-1}]$	$V_0[\text{km s}^{-1}]$
(1,1) main line	-1.4,1.4	0.08 ± 0.02	0.8 ± 0.2	-7.4 ± 0.1
	0.0,1.4	0.35 ± 0.02	0.91 ± 0.07	-7.82 ± 0.03
	1.4,1.4	0.07 ± 0.01	1.6 ± 0.4	-8.2 ± 0.2
	-1.4,0.0	0.17 ± 0.02	0.9 ± 0.1	-7.70 ± 0.05
	0.0,0.0	0.95 ± 0.04	1.04 ± 0.06	-8.08 ± 0.03
	1.4,0.0	0.18 ± 0.02	0.9 ± 0.1	-8.24 ± 0.05
	-1.4,-1.4	0.22 ± 0.02	1.1 ± 0.1	-7.72 ± 0.04
	0.0,-1.4	0.73 ± 0.03	0.97 ± 0.06	-8.07 ± 0.02
	1.4,-1.4	0.33 ± 0.02	0.85 ± 0.08	-8.21 ± 0.03
	-1.4,-2.8	0.11 ± 0.03	0.8 ± 0.3	-8.1 ± 0.1
	0.0,-2.8	0.08 ± 0.03	0.8 ± 0.3	-8.0 ± 0.1
	1.4,-2.8	≤ 0.04	-	-
(1,1) left i.s.l.	0.0,0.0	0.41 ± 0.06	1.1 ± 0.2	-15.72 ± 0.09
(1,1) right i.s.l.	0.0,0.0	0.42 ± 0.07	0.9 ± 0.2	-0.51 ± 0.08
(2,2) main line	0.0,0.0	0.17 ± 0.01	0.79 ± 0.07	-8.06 ± 0.03

TABLE I: Antenna temperature T_A , line width (FWHM) ΔV and position V_0 for $(J, K) = (1, 1)$ and $(J, K) = (2, 2)$ transition lines. Each line is identified by the corresponding transition, if it is a main or an interior satellite line (i.s.l.) and its relative position $R.P.$ with respect to the central one.

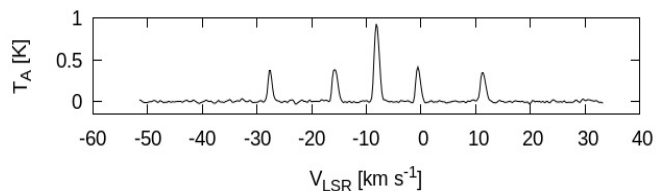


FIG. 1: Central position spectrum for the $(1, 1)$ transition.

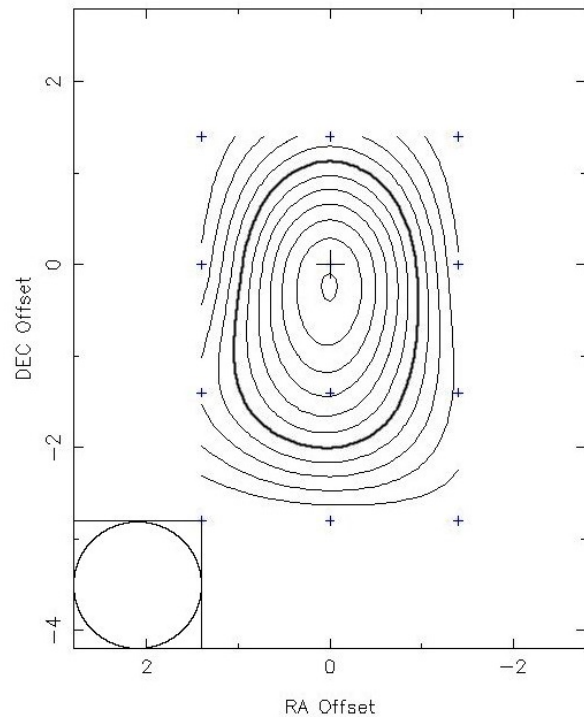


FIG. 2: Contour map of the half peak antenna temperature of the $(J, K) = (1, 1)$ inversion transition main line in the dense core of L1228. The axes indicate the offset of right ascension RA and declination DEC (in arcmin) with respect to the central position $\alpha(J2000) = 20^{\text{h}}57^{\text{m}}13^{\text{s}}.2$, $\delta(J2000) = +77^{\circ}35'46''$. The lowest contour is 0.02 K and the increment 0.04 K. The half peak intensity level is shown in bold. The observed positions are indicated with small crosses. The half power beam width of the telescope is shown as a circle. The position of the IRAS source is shown as a big cross.

REFERENCES

- [1] Anglada G., Estalella R., Mauersberger R., Torrelles J.M. et al. "The molecular environment of the HH 34 system". *The Astrophysical Journal* **443**: 682-697 (1995)
- [2] Anglada G. "Radio Jets in Young Stellar Objects". *Radio emission from the stars and the sun. Astronomical Society of the Pacific Conference Series*, **Vol. 93** (1996), (A.R.Taylor and J.M.Paredes eds.)
- [3] Anglada G., Sepúlveda I., Gómez J.F.. "Ammonia Observations towards molecular and optical outflows". *Astronomy and Astrophysics Supplement Series* **121**: 255-274 (1997)
- [4] Bally J., Devine D., Fesen R.A., Lane A.P.. "Twin Herbig-Haro jets and molecular outflows in L1228". *The Astrophysical Journal* **454**: 345-360 (1995)
- [5] Devine D., Bally J., Chiriboga D., Smart K.. "Giant Herbig-Haro flows in L1228: a second look?". *The Astronomical Journal* **137**: 3993-4001 (2009)
- [6] R. Estalella, G. Anglada, *Introducción a la física del medio interestelar*, (Publicacions i Edicions UB, 2007)
- [7] Estalella R., private communication (2013)
- [8] Narlikar J.V., *An introduction to cosmology*, (Cambridge University Press, 2002)
- [9] <http://physics.nist.gov/constants>
- [10] Sepúlveda I., "Estudio en NH_3 de regiones de formación estelar", Bachelor thesis, 1993, Universitat de Barcelona
- [11] Sepúlveda I., Anglada G., Estalella R., López R. et al.. "Dense gas and the nature of outflows". *Astronomy and Astrophysics* **A41** (2011)
- [12] Tafalla M., Myers P.C.. "Velocity shifts in L1228: the disruption of a core by an outflow". *The Astrophysical Journal* **491**: 653-662 (1997)